From Sideward Flow to Nuclear Compressibility

Qiubao Pan and Paweł Danielewicz
National Superconducting Cyclotron Laboratory and Department of Physics and Astronomy, Michigan State University, East Lansing, Michigan 48824
(Received 23 December 1992; revised manuscript received 16 March 1993)

We show that the differences between the Plastic Ball and DIOGENE experiments on sideward flow make it possible to assess independently, within the transport description of collisions, the effects of density dependence and momentum dependence of the nucleon optical potential. We estimate that the nuclear compressibility K lies between 165 and 220 MeV.

PACS numbers: 25.75.+r, 21.65.+f, 24.10.−i

Determination of the nuclear equation of state (EOS) in high-energy heavy-ion reactions turned out to be more difficult than was anticipated. It appeared possible to describe early single-particle observables using the cascade model [1] with an ideal-gas EOS lacking the potential energy term needed for binding nuclei. The importance of the mean potential felt by nucleons for the reaction dynamics was finally demonstrated when attempting to describe the observables from 4π measurements [2–4] that characterized the collective sideward flow. However, the features of the mean potential field remained ambiguous, as the magnitude of the flow represented by measured flow angles or transverse momenta could be reproduced by transport calculations utilizing potentials with either strong density or strong momentum dependence [5, 6]. Although the nonlocality of the optical potential has been long known from elastic nucleon scattering, it was never demonstrated in heavy-ion collisions. Further ambiguities were associated with the effective NN cross sections in calculations. Intuitively, the cross sections could be expected to be lower, rather than higher, than those in free space. As such, they could yield less flow [7]. Besides the flow, however, the cross sections also affect the rapidity and energy spectra, and data for the latter may be used [8] to limit the possible deviations of NN cross-section values from values in free space. The sideward flow is known to be less sensitive to NN cross sections for momentum-dependent than for momentum-independent potentials [9].

The purpose of this Letter is to show that differences between experiments investigating the dependence of sideward flow on multiplicity [10, 11] can be exploited in a transport description to assess, independently, the effects of momentum and density dependence of the optical potential on the flow. A prime source of uncertainty in the determination of nuclear compressibility becomes, in consequence, uncertainty in the NN cross sections.

Our transport model of heavy-ion collisions is based on a set of equations [12] for nucleons, nucleon resonances, and pions,

$$\frac{\partial f_a}{\partial t} + \frac{\partial \mathcal{E}_a}{\partial \mathbf{p}_a}\cdot\frac{\partial f_a}{\partial \mathbf{x}} - \frac{\partial \mathcal{E}_a}{\partial \mathbf{x}}\cdot\frac{\partial f_a}{\partial \mathbf{p}_a} = \mathcal{K}_a^<(1\mp f_a) - \mathcal{K}_a^> f_a, \tag{1}$$

where f_a is the Wigner function, $\mathcal{E}_a$ is energy, and $\mathcal{K}_a^<$ and $\mathcal{K}_a^>$ are, respectively, the production and absorption rates of the particle a. An optical potential in the baryon energies is parametrized in a local frame where the spatial component of the baryon 4-vector current,

$$j^\mu = (\rho, \mathbf{j}) = \sum_a (\rho_a, \mathbf{j}_a) = \sum_a \left(\frac{g_a}{(2\pi)^3}\int d^3p_a\, f_a, \frac{g_a}{(2\pi)^3}\int d^3p_a \frac{\partial \mathcal{E}_a}{\partial \mathbf{p}_a} f_a \right), \tag{2}$$

vanishes. The factor g_a is spin degeneracy. Covariance of (2) may be verified by a direct calculation. The potential parametrization is similar to that in nonrelativistic calculations [5],

$$U_a = \mathcal{A}\frac{\rho}{\rho_0} + \mathcal{B}\left(\frac{\rho}{\rho_0}\right)^\gamma + \frac{\mathcal{C}}{\rho_0}\sum_b \frac{g_b}{(2\pi)^3}\int d^3p_b \frac{f_b}{1+\left(\frac{p_b}{\Lambda}\right)^2} + \mathcal{C}\frac{\rho}{\rho_0}\frac{1}{1+\left(\frac{p_a}{\Lambda}\right)^2} + t_3^a\frac{\mathcal{D}}{\rho_0}\sum_b t_3^b\rho_b, \tag{3}$$

where t_3^a is the third component of isospin of the particle a. Equations (1) are solved for different values of the parameters in (3), with U treated as the fourth component of a vector potential, added to particle energy in a local frame. In tests we see no appreciable difference in our results when treating U as a scalar potential, added to mass, for the same parameter values.

Parameters in (3) are constrained by requiring that the energy per nucleon in cold symmetric matter has a minimum of $E/A \simeq -16$ MeV at $\rho_0 \simeq 0.145$ fm^{-3}. The calculations are carried out for two momentum-independent potentials ($\mathcal{C} = 0$). One of them, a soft potential referred to as S, is obtained by setting $\gamma = \frac{7}{6}$, which results in $\mathcal{A} = -348$ MeV, and $\mathcal{B} = 298$ MeV, and in the compressibility of symmetric matter $K = 199$ MeV. Another,

a hard potential, referred to as H, is obtained by setting $\gamma = 2$, which results in $\mathcal{A} = -119$ MeV, $\mathcal{B} = 68.5$ MeV, and $K = 371$ MeV. Furthermore, calculations are carried out for two momentum-dependent potentials. These potentials are required, at $\rho = \rho_0$, to yield an effective mass $m^* \simeq 0.65\,m$ at $p \simeq p_F$, and to approach $U \simeq 35$ MeV at high p. One potential, referred to as SM, is obtained by setting $\gamma = 1.06$, which results in $\mathcal{A} = -125$ MeV, $\mathcal{B} = 273$ MeV, $\mathcal{C} = -102$ MeV, $\Lambda = 526$ MeV, and $K = 176$ MeV. Another potential, referred to as HM, is obtained by setting $\gamma = 1.8$, which results in $\mathcal{A} = 107$ MeV, $\mathcal{B} = 56.5$ MeV, $\mathcal{C} = -119$ MeV, $\Lambda = 603$ MeV, and $K = 320$ MeV.

The SM potential for cold nuclear matter is compared in Fig. 1 to the potential from a microscopic calculation by Wiringa [13] using 2-nucleon UV14 and 3-nucleon UVII interactions. The potentials are fairly similar within the range of momenta and densities of interest in heavy-ion collisions. At $\rho \sim \rho_0$, the HM potential is very close to the SM potential.

The factor in the isospin term in (3) is set equal to $\mathcal{D} = 92$ MeV, in order to reproduce the asymmetry coefficient in the binding-energy formula. The Coulomb potential in our simulations is computed from the Poisson equation and added on to particle energies in the c.m. frame of a colliding system. The NN collision rates are calculated using measured cross sections unless otherwise specified. For more details on our approach see Ref. [12]. For general features of the heavy-ion collision dynamics in transport descriptions see Refs. [14–16].

Let us now turn to the data. In Figs. 2(a) and 2(b) we show (filled squares) the values of the flow parameter F from the measurements at 400 MeV/nucleon of the Nb + Nb reaction by the Plastic Ball Group [10], and of the Ar + Pb reaction by the DIOGENE Collaboration [11]. The parameter F is defined in our work as [11]

$$F = \left.\frac{d\langle p^x/m\rangle}{dy}\right|_{y_0}, \tag{4}$$

where p^x is the transverse momentum component in the reaction plane. The average is taken at a fixed rapidity y, and y_0 is the rapidity of intercept, $\langle p^x/m\rangle(y_0) = 0$. For the Nb + Nb reaction the flow parameter is presented as a function of the participant proton multiplicity N_p, and for the Ar + Pb reaction it is presented as a function of the impact parameter b estimated in the experiment. Of importance for subsequent considerations are acceptances in the experiments. The combined Plastic Ball and Wall detectors have good acceptance [10] for protons emitted in the forward laboratory direction with velocities above $0.3c$. Experimenters provide a filter program that simulates the acceptance. The data of Ref. [11] are subjected to software cuts which eliminate, in

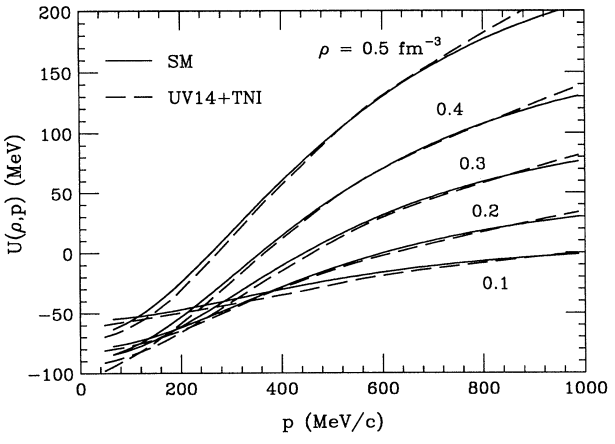

FIG. 1. The SM potential for cold nuclear matter is compared to the potential from a microscopic calculation [13] using UV14 + TNI interactions. Numbers indicate density in fm^{-3}.

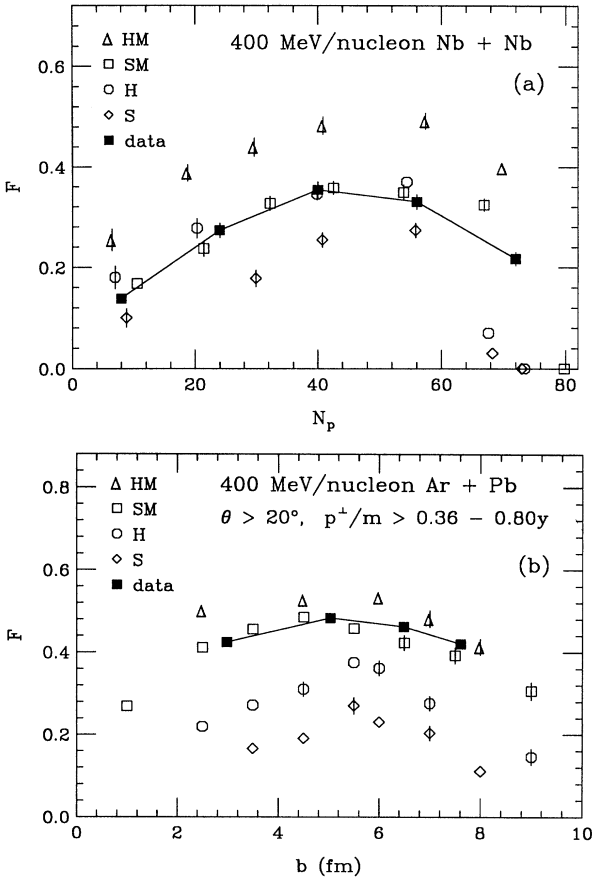

FIG. 2. Flow parameter F in (a) Nb + Nb and (b) Ar + Pb reactions at 400 MeV/nucleon. Data of Refs. [10, 11] (filled squares) are compared to the results of calculations for different optical potentials (open symbols). In (a) and (b) the abscissa shows participant proton multiplicity and impact parameter, respectively. Error bars for the results of calculations, suppressed when less than symbol size, represent uncertainties due to finite statistics.

the forward direction, the particles emitted under an angle of 20° and, further, those particles whose transverse momenta satisfy $p^{\perp}/m < 0.36 - 0.80y$.

Besides the results of measurements, we show in Fig. 2 the results of our transport-model calculations (open symbols) for the different optical potentials, with emitted protons subjected to the acceptance filters. It is seen in Fig. 2 that calculations utilizing potential S generally underpredict the measured flow values, the calculations utilizing potential H quite clearly underpredict measured values in Ar + Pb reaction, while those utilizing potential HM overpredict the flow values in the Nb + Nb reaction. Only calculations utilizing potential SM conform, to a reasonable extent, with data for either of the reactions.

The differences between the predictions of calculations utilizing SM and H potentials, present at all b in the Ar + Pb reaction, are startling; just as startling is the failure of calculations utilizing potential H to reproduce the data. In past studies [5, 6, 15], and for the Nb + Nb reaction, the two types of potentials gave similar results for the same b. While some differences between the predictions for the Ar + Pb reaction are present prior to the application of acceptance cuts (predictions based on two types of potentials were never compared for strongly asymmetric systems), the differences are more than doubled by the cuts. The effect may be understood by examining Fig. 3. In this figure we show, as a function of transverse momentum, the average values of cosine of the azimuthal angle with respect to reaction plane, of nucleons emitted at $y > y_0$ from $b = 4.5$ fm reaction, for the different potentials. It is seen that particles with high $p^{\perp}$ are much more focused at one side of the beam axis in the vicinity of the reaction plane for momentum-dependent than for momentum-independent potentials. Indeed, in the case of a momentum-dependent potential, the particles with high momenta are subjected to an enhanced repulsion in the central region of a reaction. When an analysis is limited to particles emitted with high $p^{\perp}$, the flow values for a potential dependent on momentum rise relative to the flow values for a momentum-independent potential.

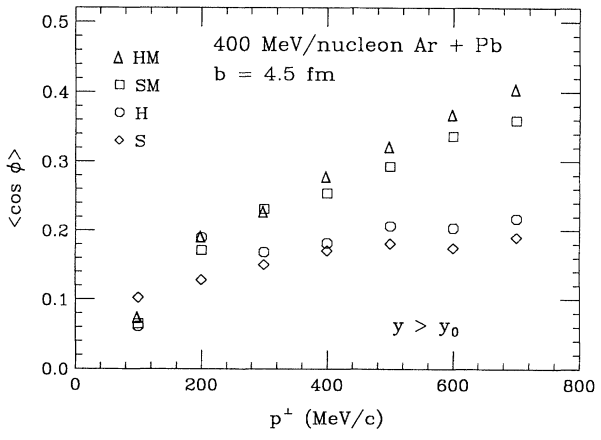

FIG. 3. Mean cosine of the azimuthal angle with respect to the reaction plane, of nucleons emitted at $y > y_0$, as a function of the nucleon transverse momentum.

From the two data sets, the Ar + Pb data set better constrains the momentum dependence of the optical potential, while the Nb + Nb set better constrains the density dependence. For $p/\Lambda \lesssim 1$, the dependence of the potentials (3) on p is controlled by C/Λ^2, or simply m^* at $\rho = \rho_0$. Using data one might consider carrying out a χ^2 optimization in the space of m^* and K. However, from Fig. 2 it follows that one is relatively close to a minimum of χ^2 for the functional form (3), with the parameters SM. (Moderate adjustments to the SM parameters were done prior to deciding on the values to be used; possibly m^* requires finer adjustment.) Another issue that needs to be addressed is whether optimization at other beam energies might yield different parameters. Discrepancies could indicate an inadequacy of the assumed form of the potential, and, in particular, an improper power of ρ/ρ_0 in the momentum-dependent term in U, Eq. (3). With the power of density ratio in that term made a free parameter, using data on flow in heavy-ion collisions with and without low $p^{\perp}$ cuts, over a range of bombarding energies, one might attempt to determine not only an optimal new parameter, K, and m^*, but also an optimal Λ. The procedure would be much more time consuming than present, already intense, calculations. Fortunately, it appears that, with the present potential form and the parameters SM, one must be relatively close to the possible outcome of an extended optimization procedure as well. Predictions based on the SM potential agree to a reasonable extent with the DIOGENE data on the variation of flow with b in the Ne + Pb reaction at 800

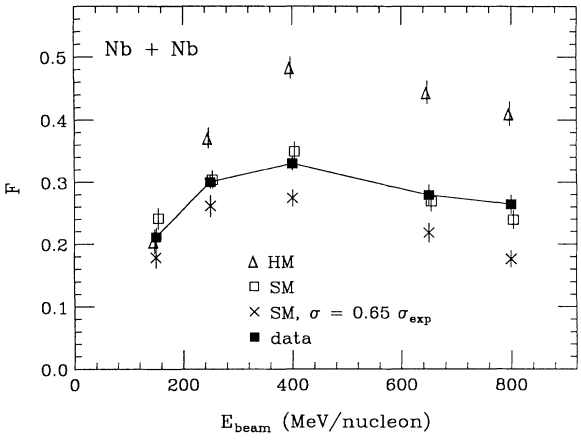

FIG. 4. Flow parameter in the Nb + Nb reaction as a function of beam energy. Experimental values (filled squares) for the fourth bin of reduced multiplicity [11], $N_p/N_p^{\max} \simeq 0.88$, are compared to the results of calculations at $b = 4.5$ fm for HM potential (open triangles), SM potential (open squares), and SM potential and the cross sections reduced by 35% (crosses).

MeV/nucleon [11], and also with the Streamer Chamber data [17] on the variation of $\langle p^x/A \rangle$ with y in the semicentral Ar + Pb events at that bombarding energy. In Fig. 4, good agreement can be seen between the calculated and measured flow values at several bombarding energies in the Nb + Nb reaction, at a fixed reduced multiplicity [10]. Other systems where consistency between the SM predictions and data was found include Au + Au and Ca + Ca at 400 MeV/nucleon [10].

It is important to consider an effect on the conclusions concerning K, of the possible reduction of cross sections in the medium. A comparison of the calculated and measured rapidity distributions in the reactions at 400 and 800 MeV/nucleon [17, 18] excludes an overall reduction of the elementary cross sections by more than $\sim$ 35% relative to free space at the high energies, but not by a lesser amount. An effect of the 35% reduction on the flow parameter in calculations utilizing the SM potential is illustrated in Fig. 4. An acceptable agreement with the Nb + Nb and Ar + Pb data, for the reduced cross sections, is obtained when K is raised to 205 MeV, with potential parameters following from such constraints as before. Of concern might be the effect of composite production on the flow. However, we found this effect negligible when treating the production as in Refs. [12, 16], and calculating the flow before or upon an application of the acceptance filters. Using the behavior of our predictions with K, m^*, and cross sections, and the actual deviations of the SM predictions from data, and further taking into account some uncertainty associated with the form of a potential, we estimate that nuclear compressibility lies between 165 and 220 MeV.

The authors thank C. Gale and J. Zhang for fruitful discussions and for pointing out a mistake in the first version of the manuscript, and S. Pratt for suggestions concerning the text. This work was partially supported by the National Science Foundation under Grant No. PHY-9017077.

[1] Y. Yariv and Z. Frankel, Phys. Rev. C **20**, 2227 (1979); J. Cugnon, *ibid.* **22**, 1885 (1980).
[2] H. A. Gustafsson *et al.*, Phys. Rev. Lett. **52**, 1590 (1984); R. E. Renfordt *et al.*, *ibid.* **53**, 763 (1984).
[3] P. Danielewicz and G. Odyniec, Phys. Lett. **157B**, 146 (1985).
[4] K. G. R. Doss *et al.*, Phys. Rev. Lett. **57**, 302 (1986).
[5] C. Gale *et al.*, Phys. Rev. C **35**, 1666 (1987).
[6] J. Aichelin *et al.*, Phys. Rev. Lett. **58**, 1926 (1987).
[7] G. F. Bertsch *et al.*, Phys. Lett. B **189**, 384 (1987).
[8] J. Jiang *et al.*, Phys. Rev. C **43**, 2353 (1991).
[9] G. M. Welke *et al.*, Phys. Rev. C **38**, 2101 (1988).
[10] H. Å. Gustafsson *et al.*, Mod. Phys. Lett. A **3**, 1323 (1988).
[11] M. Demoulins, Ph.D. thesis, University Paris Sud, 1989 [CEN Saclay Report No. CEA-N-2628, 1990 (unpublished)]; J. Gosset *et al.*, in *The Nuclear Equation of State*, edited by W. Greiner and H. Stöcker, NATO ASI Ser. A, Vol. 216 (Plenum, New York, 1989), p. 87; M. Demoulins *et al.*, Phys. Lett. B **241**, 476 (1990).
[12] P. Danielewicz and G.F. Bertsch, Nucl. Phys. **A533**, 712 (1991).
[13] R. B. Wiringa, Phys. Rev. C **38**, 2967 (1988).
[14] J. J. Molitoris *et al.*, Phys. Rev. C **36**, 220 (1987); B. Blättel *et al.*, *ibid.* **43**, 2728 (1991).
[15] C. Gale *et al.*, Phys. Rev. C **41**, 1545 (1990).
[16] P. Danielewicz and Q. Pan, Phys. Rev. C **46**, 2002 (1992).
[17] D. Beavis *et al.*, Phys. Rev. C **45**, 299 (1992).
[18] H. H. Gutbrod *et al.*, Z. Phys. A **337**, 57 (1990).